

Determination of Interfacial Tension Between PA/PP and LCP/PP by IFR Method and Effect of Compatibilization on Interfacial Tension

J. KIRJAVA,^{1*} T. RUNDQVIST,² R. HOLSTI-MIETTINEN,¹ M. HEINO,¹ and T. VAINIO¹

¹Helsinki University of Technology, Department of Chemical Engineering, Kemistintie 1, FIN-02150 Espoo, Finland and ²Lund Institute of Technology, Department of Production and Materials Engineering, P.O. Box 118, S-22100 Lund, Sweden

SYNOPSIS

The dynamic imbedded fiber retraction (IFR) method was used to measure the interfacial tension between two molten polymers. The aim was to evaluate the applicability of this method for polypropylene (PP) used as matrix, and two polyamide (PA6, PA66) and thermotropic main-chain liquid crystalline polymer fibers. The effect on the interfacial properties of modifying the PP matrix with compatibilizers was studied as well. The IFR method was found to be suitable for evaluating the interfacial properties of these polymer blends. The measured interfacial tensions correlated well with the morphology and mechanical properties of the blends and values calculated from the harmonic mean equation. Although the measured interfacial tensions were generally lower than the theoretical ones, the order of the values for the different polymer pairs was similar. © 1995 John Wiley & Sons, Inc.

INTRODUCTION

Properties of immiscible polymer blends depend on the flow induced morphology formed during blending and processing. In the research on these blends much attention has been paid to the rheological properties of the components, blend composition, and processing parameters, as factors determining the macroscopical properties of the blends. By contrast, only limited attention has been focused on the interfacial forces, which equally influence the blend properties.^{1,2} One of the reasons for this neglect is that few reliable methods exist for measuring the interfacial forces acting between two polymers in the melt state.

The interfacial tension between the two phases of an immiscible polymer blend is generally high, resulting in a clear two-phase morphology with large spherical droplets of the dispersed phase and sharp phase boundaries. The interfacial tension is based

on the chemical characteristics of the blended polymers; in particular the difference in polarity between the two phases is of importance.³ Other relevant factors are molecular weight, temperature, and possible additives. The interfacial tension between blend components can be reduced through the addition of suitable compatibilizers such as block or graft copolymers.⁴

Chen et al.⁵ measured the interfacial tension by the pendant drop method in four different systems: polyethylene/polystyrene (PE/PS), PE/polyamide 6 (PA6), PS/polyethylene terephthalate (PET), and PS/PA6. Similar blends with potential compatibilizers were studied as well, and a decrease in the interfacial tension was observed in the presence of various graft and block copolymer compatibilizers. Hobbs et al.⁶ utilized the interfacial forces for the formation of complicated encapsulated morphologies in blends of at least three polymers.

In this work we applied the dynamic method developed by Carriere et al.⁷ for measuring the interfacial tension between two polymer melts. The method involves monitoring the retraction of an imbedded fiber (imbedded fiber retraction, IFR

* To whom correspondence should be addressed.

method). So far, the IFR method has been used for PS/poly(methylene methacrylate) (PMMA),^{7,8} polycarbonate (PC)/PMMA,⁹ and poly(styrene/acrylonitrile/fumaronitrile [poly(S/AN/FN)]/poly(S/AN)).¹⁰ The results showed it to be a promising method for studying the composition-dependent compatibility of blends: as the molecular miscibility increases, the interfacial tension decreases.¹⁰

In our earlier investigations of the compatibilization of PA/polypropylene (PP)¹¹ and LCP/PP blends,¹² results of differential scanning calorimetry (DSC), dynamic mechanical thermal analysis (DMTA), Fourier transform infrared spectroscopy (FTIR), and morphological analysis clearly indicated enhanced interactions between the blended polymers when certain compatibilizers were present. The interfacial adhesion between the two molten polymers was not, however, measured for lack of a proven method. The aim of this work was to determine whether the IFR method could be used to measure the interfacial tensions between these partially crystalline polymers. Of particular interest to us was the effect of compatibilizers on the interfacial properties. The method was evaluated in two ways: by correlating the results with the morphology and macroscopic properties of the corresponding blends and by comparing the measured interfacial tensions with values calculated from the harmonic mean equation, a theoretical expression based on the surface tensions and work of adhesion of the components.

IFR METHOD

The IFR method is a dynamic method for measuring the interfacial tension between two high molecular weight polymers in the molten state. The method involves the microscopic tracking of the shape evolution of a short imbedded fiber and uses interfacial tension as a driving force for the retraction process. The retraction rate depends on the interfacial tension, viscosities of the materials, and volume and geometry of the fiber. The method was developed because the standard equilibrium methods were unable to measure the interfacial tension between high viscosity polymers.⁷

The major disadvantages of the equilibrium methods are that a long time may be required to reach equilibrium and it is difficult to determine when that equilibrium has been reached. During the time required for the measurement, thermal degradation of the materials may occur.

In the IFR technique, measurement takes place

during the relatively short retraction process, and if thermal degradation or other disturbances occur during the retraction process the measurement up to that point can be considered adequate.

A major requirement of the method is that the matrix material be transparent in the molten state. It should also have a lower melting point than the fiber material in order that flattening of the fiber does not occur during the imbedding process.

The method is based on the balance between the interfacial and viscous forces at the fiber/matrix interface expressed as⁸:

$$6\pi\chi R(t)\eta_e \frac{1dL}{2dt} = -\gamma_{12} \frac{dA}{dL} \quad (1)$$

where χ is a hydrodynamic coefficient, $R(t)$ is the effective radius of the fiber, η_e the effective viscosity, L the length of the fiber, γ_{12} the interfacial tension between polymers 1 and 2, and A the interfacial area. The model assumes that during the retraction process the fiber is a cylinder with hemispherical caps and an effective radius R . The effective radius R at time t is determined as the radius of a cylinder having equal volume and length as the retracting fiber. In the end, the fiber will retract into the form of a sphere with a radius R_0 . A dimensionless radius $r(t)$ is used in the calculations⁸:

$$r(t) = \frac{R(t)}{R_0} \quad (2)$$

The effective viscosity is expressed as⁸:

$$\eta_e = \frac{\eta_m + 1.7\eta_f}{2.7} \quad (3)$$

where η_m and η_f are the viscosities of the matrix and fiber material, respectively. The hydrodynamic coefficient is assigned to be constant ($\chi = 1$). The expression (3) and coefficient χ are empirical and based on measurements made with PS and PMMA,⁸ but they are assumed to be valid for the combinations of materials used. Because the deformation rate during the measurement is low (10^{-4} – 10^{-3} s⁻¹), the zero-shear viscosities of the polymers are used in the calculations.

For the determination of interfacial tension, the function $f[r(t)] - f[r(0)]$ is plotted vs. time (t) and the interfacial tension is obtained from the slope of the linear part of the curve⁹:

$$f[r(t)] - f[r(0)] = t \frac{\gamma_{12}}{R_0\eta_e} \quad (4)$$

where the function f is expressed as⁹:

$$f(x) = \frac{3}{2} \ln \frac{\sqrt{1+x+x^2}}{1-x} + \frac{3^{1.5}}{2} \arctan\left(\sqrt{3} \frac{x}{2+x}\right) - \frac{x}{2} - \frac{4}{x^2}. \quad (5)$$

The slope is calculated by the linear fit of the measured points with the least-squares method (Fig. 1). Note that only the linear part of the curve can be used for the calculations. The curve usually contains two parts that should not be used: the first part of the curve, where deviations from the linear behavior may be due to the settlement of the materials and thermal nonequilibrium, and the final part of the curve, where thermal degradation of the materials may have an effect.

EXPERIMENTAL

Materials

The matrix material was PP VB65 50B, an isotactic homopolymer produced by Neste. According to the manufacturer it has a M_w of 275,000 g/mol, a M_n of 57,000 g/mol, and a melt index of 6.5 g/10 min (230°C/2.16 kg). The fiber materials were two polyamides, PA6 (Ultramid B3S) and PA66 (Ultramid A3K), both produced by BASF, and two liquid crystalline polymers, LCP1 (Vectra A950 from Hoechst Celanese) and LCP2 (Rodrun LC-3000 from Unittika). Both LCPs are thermotropic main-chain copolyesters.

Vectra A950 is a copolymer of *p*-hydroxybenzoic acid (HBA) and 6-hydroxy-2-naphthoic acid (HNA).

The following specifications are given by the manufacturer: density 1.4 g/cm³, melting temperature 280°C, tensile strength 165 MPa, elastic modulus 9700 MPa, and elongation at break 3.0%.

Rodrun LC-3000 is a more flexible copolyester consisting of 60% HBA and 40% PET. The following properties are given by the manufacturer: density 1.4 g/cm³, melting temperature around 210°C, tensile strength 118 MPa, flexural modulus 9300 MPa, and elongation at break 5.0%.

The effect of compatibilization was studied by using two functionalized PP matrices, hereafter referred to as MOD1 and MOD2. MOD1 is a blend achieved by adding 5 wt % of an ethylene-based reactive terpolymer (Lotader AX-8660 from Atochem) to the PP homopolymer. MOD2 is a maleic anhydride grafted PP (PP-*g*-MAH) with 0.4 wt % of maleic anhydride (MAH) (Exxelor PO X1 1015 from Exxon). It has a melt index of 120 g/10 min (230°C/2.16 kg).

Preparation of IFR Samples

The fibers for the measurements were prepared with a Göttfert Rheograph 2002 capillary viscosimeter using a die with L/d (length/diameter) ratio of 20/0.5 or 30/1. The shear rates ranged from 50 to 4000 1/s. Fibers were extruded with or without additional drawing, which gave final draw ratios of 1.1–16.

Matrix materials were injection molded with an Engel ES 200/40 injection molding machine or compression molded with Fontijne Holland TP 400 equipment. The dimensions of the injection and compression molded plates were 100 × 100 × 2 mm and 200 × 200 × 3 mm, respectively. All materials

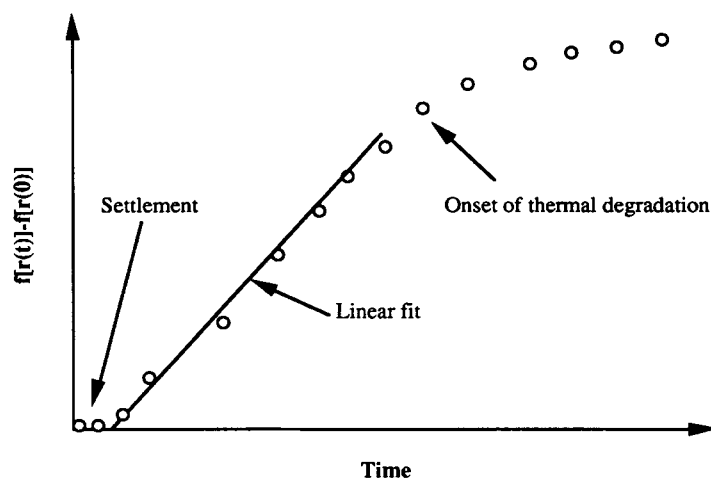


Figure 1 An example of the plot $f[r(t)] - f[r(0)]$ vs. time (t).

were dried before processing and processed at conditions recommended by the manufacturers.

The blend MOD1 was made with a Brabender DSK 42/7 counter-rotating twin-screw extruder and subsequently injection or compression molded to plates as described above.

Matrix disks 20 mm in diameter were punched out from the injection or compression molded plates with a hydraulic press. Before measurement all materials were dried at 80–90°C for 16 h.

Viscosity Measurements

The viscosities of both fiber and matrix materials were measured with a Weissenberg rheogoniometer, using Carrimed60 software for analysis. The measurements were performed in torsional flow using parallel plates 40 mm in diameter. The gap between the plates was 1–1.5 mm. Because the shear rates were low, the measured viscosities remained in the Newtonian region and could thus be treated as zero-shear viscosities. Three to five measurements were carried out for each material.

Annealing and Fiber Dimensions

The fibers were prepared with a viscosimeter and some of them were exposed to high draw ratios and shear rates. Some of the fibers prepared of LCP2 were annealed before measurement, to remove possible residual stresses that might affect the measurement. Annealing was carried out in a vacuum oven at 230°C for 5–10 min.

The most suitable fiber length and diameter were selected individually for each fiber-matrix pair. The zero-shear viscosities of both the fiber and matrix materials, and thus their viscosity ratio (η_f/η_m), were taken into account when deciding upon the fiber di-

mensions. If the viscosity ratio was high, fibers with higher L/d ratios could be used without breakup of the fiber. L/d ratios of the fibers thus varied between 6 and 11.

Imbedding

Before measurement the fiber was cut to suitable length under a microscope, positioned between two matrix disks in a glass container, and the whole placed in a vacuum oven at 190–200°C for 20–60 min. In the oven the matrix material melted around the fiber, imbedding it.

To avoid or minimize thermal degradation the samples were kept in the imbedding oven for the shortest possible time, that is, only as long as required to melt the matrix material. After imbedding, the samples were placed directly into the tube furnace (oven).

Equipment and Measurement Procedure

The experimental IFR apparatus is depicted in Figure 2. The sample was placed into a tube furnace with an inspection window on the top. The temperature was controlled by a PID regulator and the temperature of the sample was measured with a thermocouple. To remove oxygen, and so hinder degradation of the sample, a constant preheated nitrogen gas flow was fed into the furnace.

The sample was illuminated with two point-lights with flexible shafts and the retraction process was tracked with a stereomicroscope (Nikon SMZ-2T) rebuilt to have six fixed magnification levels varying from 10 to 60. The image was displayed on a monitor by a video camera, and pictures could be printed out at preselected time intervals. The magnification of the printouts was calibrated with a micrometer.

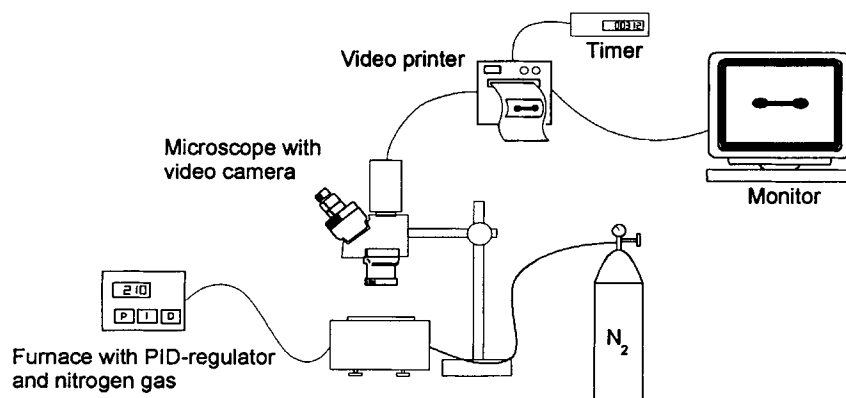


Figure 2 Description of the experimental apparatus.

Sample Preparation for Morphology Studies

Morphology studies were done on compatibilized and noncompatibilized PP/PA6, PP/PA66, and PP/LCP2 melt blends. The compatibilizer was the same reactive ethylene-based terpolymer as in MOD1, present in a concentration of 5 wt %. Blending was made with a Werner & Pfleiderer ZSK 25 M9 co-rotating twin-screw extruder at melt temperatures of 250°C for PA6/PP and LCP2/PP and 280°C for PA66/PP. The extrudate was immediately quenched in a water bath and free fallen strands were taken for morphology studies.

Characterization of Blend Morphologies

Morphologies of the blend samples were investigated with a JEOL JXA-840A scanning electron microscope (SEM). The samples were fractured after liquid nitrogen cooling. Before scanning, the fracture surfaces were plated with a thin layer of gold.

DSC Analysis

To investigate the effect of possible thermal degradation during the IFR measurement, matrix disks were analyzed by DSC using Mettler DSC-30 equipment. Samples were cut from three different layers of the disk. The heating and cooling rates were 20°C/min.

RESULTS AND DISCUSSION

Viscosity Measurements

The polymer pairs for this research were selected on the basis of the results of our earlier studies¹³ so that viscosity ratios in the processing conditions applied were suitable for the melt processing ($\eta_f/\eta_m = 0.5-1$). However, when zero-shear viscosities are considered, the viscosity ratios of some of the pairs were nevertheless far from optimal. The measured

Table I Zero-Shear Viscosities (η_0) of Fiber Materials at Their Measuring Temperatures

Material	T (°C)	η_0 (Pa·s)
LCP1	310	5860 ± 640
LCP2	250	450 ± 70
PA6	250	110 ± 10
PA66	280	140 ± 10

Table II Zero-Shear Viscosities (η_0) of Matrix Materials

Material	η_0 (Pa·s)		
	250°C	280°C	310°C
PP	1240 ± 90	610 ± 30	110 ± 10
MOD1	1010 ± 20	570 ± 10	—
MOD2	60 ± 5	—	—

zero-shear viscosities of the fiber and matrix materials are presented in Tables I and II.

Interfacial Tension Between Pure Polymers

Table III shows the interfacial tensions between PP and the four fiber materials (LCP1, LCP2, PA6, and PA66) measured by the IFR method, together with the viscosity ratio for each pair.

Polyamides were measured at their normal processing temperatures (PA6 250°C, PA66 280°C), and LCPs at about 20°C higher than their normal processing temperatures (LCP1 310°C, LCP2 250°C). LCPs did not melt at their normal processing temperatures, evidently because, during the measurement, no shearing was applied to the fiber.

The interfacial tension between LCP1 and PP was surprisingly low compared with the other pairs, probably due to the extremely high ratio of zero-shear viscosities of LCP1 and PP. The effective viscosity is an empirical expression determined in the viscosity ratio range of 0.1–10.⁸ It might not be valid for ratios as high as 50 (LCP1/PP). In addition the high measuring temperature (310°C) might have some influence on the interfacial tension.

Annealing experiments were made to study the possible relaxation of the highly drawn fibers. No changes in the fiber dimensions were found however, and thus annealing was not needed before the IFR measurement.

Table III Interfacial Tensions and Viscosity Ratios Between Fiber Materials and PP

Fiber	γ_{12} (mN/m)	T (°C)	η_f/η_m
LCP1	1.29 ± 0.09	310	53
LCP2	5.90 ± 0.34	250	0.37
PA6	7.84 ± 0.44	250	0.09
PA66	5.62 ± 0.34	280	0.25

Measured by the IFR method.

The standard deviations were small and the reproducibility of the measurements was good.

Comparison of Measured and Calculated Values

The interfacial tension between PP and the fiber materials (LCP1, LCP2, PA6, and PA66) was calculated by the harmonic mean equation, which is written as follows¹⁴:

$$\gamma_{12} = \gamma_1 + \gamma_2 - \frac{4\gamma_1^d\gamma_2^d}{\gamma_1^d + \gamma_2^d} - \frac{4\gamma_1^p\gamma_2^p}{\gamma_1^p + \gamma_2^p} \quad (6)$$

where γ_{12} is the interfacial tension between components 1 and 2, γ_i is the surface tension of component i , γ_i^d is the dispersive part of the surface tension of component i , and γ_i^p is the polar part of the surface tension of component i .

The values used in calculations are presented in Table IV. From the values in Table IV, the following interfacial tensions were obtained by the harmonic mean equation:

$$\begin{aligned} \gamma_{PP/LCP1} &= 10.32 \text{ mN/m} && \text{(at } 310^\circ\text{C)} \\ \gamma_{PP/LCP2} &= 10.66 \text{ mN/m} && \text{(at } 250^\circ\text{C)} \\ \gamma_{PP/PA6} &= 13.34 \text{ mN/m} && \text{(at } 250^\circ\text{C)} \\ \gamma_{PP/PA66} &= 9.91 \text{ mN/m} && \text{(at } 280^\circ\text{C)}. \end{aligned}$$

The measured values, shown in Table III, were generally lower than the calculated ones, but, disregarding LCP1, the order of the values for the different polymer pairs was the same. The materials used in the measurements were commercial grades containing additives that might be partly responsible for the lower interfacial tensions. The measured interfacial tension between PP and LCP1 was much lower than expected from the calculations. Probably

this was due to the exceptionally high viscosity ratio of LCP1 to PP. It should be noted that the IFR method has so far been applied to polymer pairs with viscosity ratios close to unity. The viscosities of the other three fiber materials were similar to each other.

In addition, the measurement of zero-shear viscosity of LCP1 was difficult, because it has no Newtonian region but is extremely pseudoplastic even at low shear rates. This was reported also by Guskey and Winter.¹⁹

In spite of the long measurement times and possible thermal degradation, the IFR method gave reproducible results with small standard deviations. The interfacial properties of the materials studied could be characterized, as was hoped. As we see below, the results of the IFR studies also correlated well with the morphology of the blends.

Effect of Compatibilizing Agents on Interfacial Tension

The effect of compatibilizing agents on interfacial tension was studied by using MOD1 as a matrix for LCP2, PA6, and PA66 fibers and MOD2 as a matrix for LCP2. The measuring procedure was the same as that used for the pure polymers, except that shorter fibers were used than with pure PP in anticipation of the lower interfacial tension, and consequent slower retraction. The risk of greater thermal degradation with longer measuring time was in that way diminished. The interfacial tensions between the modified PPs and the three fibers are presented in Table V.

In general, the interfacial tensions between the three fiber materials and the modified PPs were significantly lower than those obtained with the pure PP homopolymer. The MAH-grafted PP (MOD2) decreased the value by 40% relative to that obtained

Table IV Values for Calculating Interfacial Tension with Harmonic Mean Equation

Material	γ (mN/m)	x^p	γ^p (mN/m)	γ^d (mN/m)	$d\gamma/dT$ (mN/m ² °C)	Ref.
PP (250°C)	16.50	0.020	0.33	16.17	-0.056	14
PP (280°C)	14.82	0.020	0.30	14.52	-0.056	14
PP (310°C)	13.14	0.020	0.26	12.88	-0.056	14
LCP1 (310°C)	30.96	0.298	9.23	21.73	-0.053	15
LCP2 (250°C)	31.91	0.345	11.01	20.90	—	14, 16
PA6 (250°C)	37.07	0.340	12.60	24.47	-0.065	14-18
PA66 (280°C)	29.55	0.340	10.05	19.50	-0.065	14

Table V Interfacial Tensions and Viscosity Ratios Between the Fiber Materials and MOD1 and MOD2

Fiber	Matrix			
	MOD1		MOD2	
	γ_{12} (mN/m)	η_t/η_m	γ_{12} (mN/m)	η_t/η_m
LCP2 (250°C)	0.53 ± 0.18	0.45	3.64 ± 0.41	7.5
PA6 (250°C)	0.99 ± 0.17	0.11	—	—
PA66 (280°C)	0.55 ± 0.08	0.25	—	—

Measured by IFR method. (—) not measured.

for LCP2/PP. The reactive compatibilizer in MOD1 had an even more dramatic effect, decreasing the interfacial tension in all three systems by as much as 90%. The effects of the modified PPs on the interfacial tension were closely related to their effects on the morphology and properties of the blends (see below).

Correlations Between Interfacial Tension and Morphology

The morphologies of the compatibilized and noncompatibilized PP/LCP2, PP/PA6, and PP/PA66 (70/30) blends were studied to allow the effects of compatibilizers on the interfacial tension to be correlated with the effects on morphology. The morphologies of the blends are presented in Figure 3 as SEM micrographs of the cross-sections of free-fallen extrudate strands.

All three blend systems exhibited two clearly distinct phases because the blended polymers were generally immiscible. In the noncompatibilized blends the sizes of the dispersed droplets were generally about 10 μm , although large deviations existed.

The reactive compatibilizer dispersed the minor phases to significantly finer droplets and homogenized the droplet size leading to a more stabilized morphology. After addition of the compatibilizer the dispersed domains were generally only about 2–3 μm (LCP2), 1–2 μm (PA6), and 1 μm or below (PA66) in diameter. In addition to this emulsifying effect, the compatibilizer caused the dispersed phases to attach better in the matrix, which agrees well with the reduction in interfacial tension. In

noncompatibilized blends the minor phase existed as spherical domains with sharp boundaries with the matrix, an indication of high interfacial tension. In compatibilized blends the shape of the dispersed phases was more irregular and the phase boundaries were no longer so sharp. In particular, the dispersed small PA domains were well imbedded in the PP matrix.

Correlations Between Interfacial Tension and Blend Properties

Decreased interfacial tension, and thus enhanced interfacial adhesion induced by the compatibilizers, led to better attachment of the dispersed phase to the matrix. This resulted in significantly improved toughness of both PA/PP and LCP/PP blends as reported in our earlier articles. Moreover, addition of the reactive compatibilizer increased the melt viscosity of the blends referring to a possible chemical reaction between the blended polymers.^{11,12} Hence, the improved compatibility of these blends could now be evidenced by the IFR method without making the blends.

Sources of Error in IFR Method

Measurement of Zero-Shear Viscosity

One of the most critical factors in the determination of interfacial tension by the IFR method is the measurement of zero-shear viscosity.¹² As can be seen from Eq. (3), inaccuracy in the viscosity measurement of the fiber material is more critical than that of the matrix. The time needed for the measurement may sometimes be very long. In this study LCP1 required a measuring time as long as 4 h because after each change in shear rate the equilibrium was reached very slowly. Such a long time at an elevated temperature may easily lead to thermal degradation, and to inaccuracy in the measurement of viscosity and thus of interfacial tension. It should be emphasized that the determination of zero-shear viscosity of this type of LCP is difficult due to shear thinning even at low shear rates.¹⁹ For PPs, PAs, and LCP2, which all exhibited Newtonian behavior at low shear rates, the measuring times were 2–3 min, 3–5 min, and about 20 min, respectively.

Thermal Degradation

Because the measuring temperatures were much above the normal processing temperature of the PP

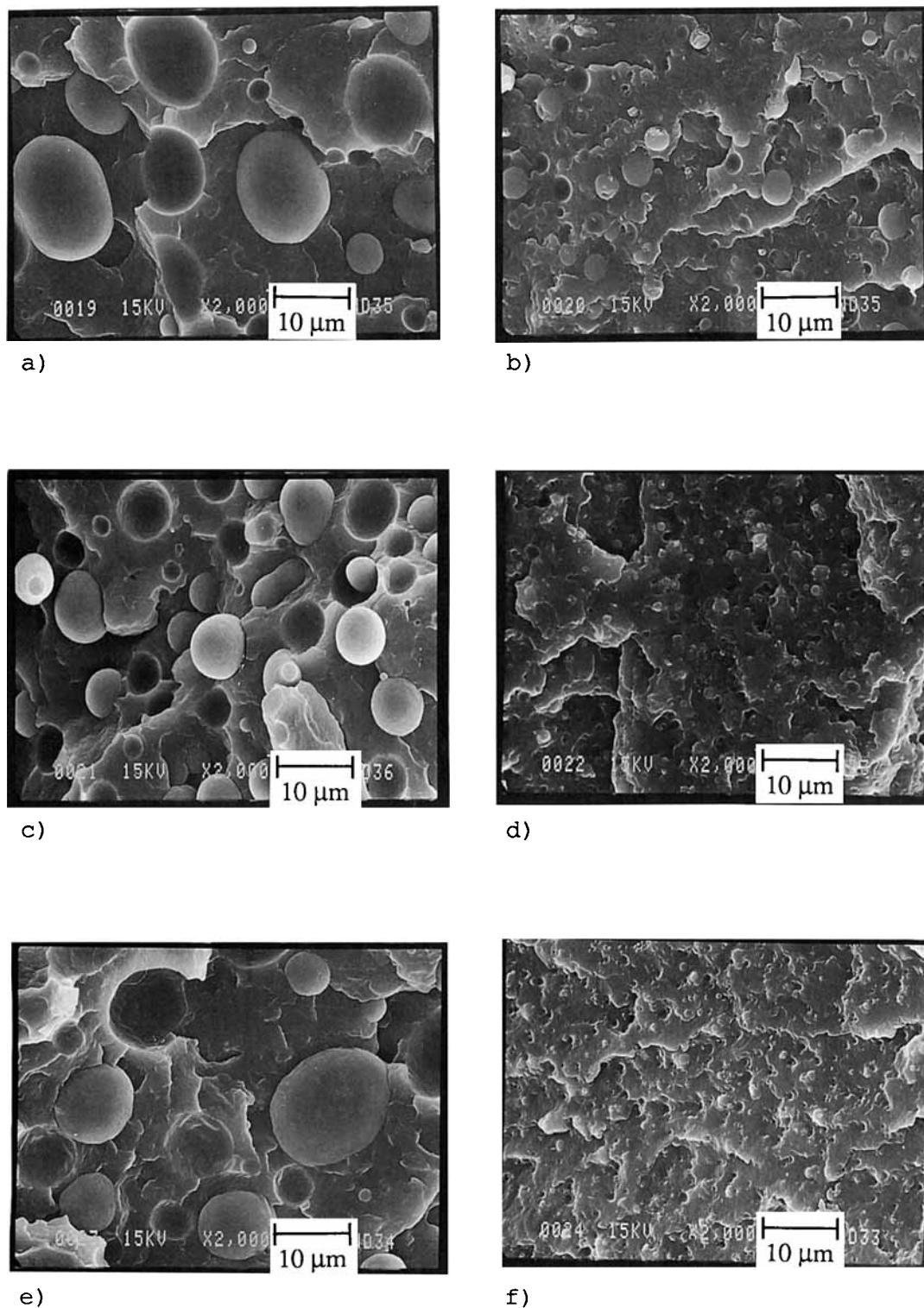


Figure 3 SEM micrographs of extruded blends (70/30): (a) PP/LCP2; (b) compatibilized PP/LCP2; (c) PP/PA6; (d) compatibilized PP/PA6; (e) PP/PA66; and (f) compatibilized PP/PA66.

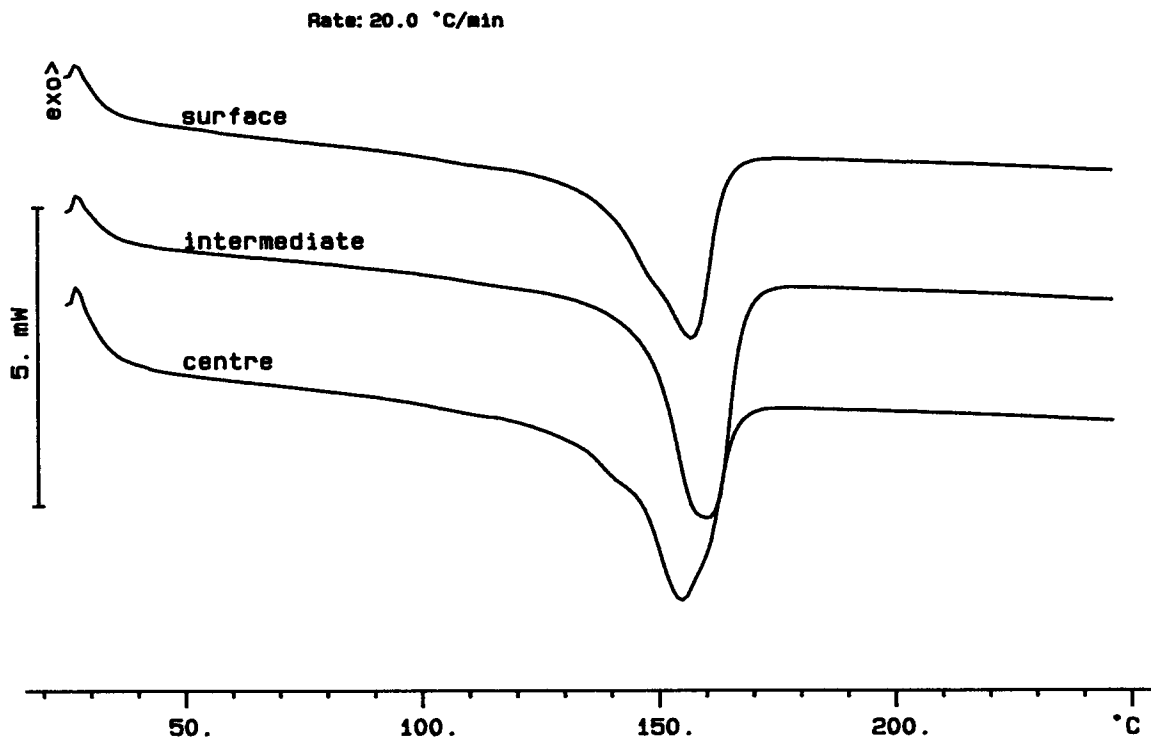


Figure 4 The DSC curve of outer surface, intermediate layer, and center section of the PP matrix disk. The thermal history of the sample was 60 min at 190°C and 45 min at 310°C.

matrix, thermal degradation of PP was likely to occur during the long time needed for the measurement. DSC analysis was applied to determine if any degradation had occurred. The DSC curves from three different layers of a matrix disk are presented in Figure 4.

The thermal history of the samples in Figure 4 was 60 min at 190°C (imbedding) and after that 45 min at 310°C (retraction). DSC analysis revealed a slight melting point depression of the PP matrix related to thermal degradation. As seen in Figure 4, the degree of thermal degradation differed in the three layers studied.

However, the total retraction is not required for the measurement of interfacial tension and reliable results can be achieved by measuring only a few points from the linear part of the retraction curve, that is, from the beginning of the retraction process. The effect of thermal degradation can thereby be minimized, and the testing procedure speeded up.⁸

Effect of Annealing

Although minor shrinkage was observed in some fibers after heating, no difference in interfacial tension

was noticed between annealed and nonannealed fibers. It can be assumed, therefore, that the required relaxation of the fibers took place in the furnace while the sample was being heated.

Measurement of Fiber Dimensions

Yet another potential source of error is the measurement of fiber dimensions during the retraction process. An error in the measured length of the fiber would give double the error in the interfacial tension, assuming that the volume of the fiber was correct (e.g. as measured with a microscope before retraction). The length may be measured inaccurately if the fiber is not in the horizontal plane after imbedding. For example, the measured interfacial tension would be about 4% smaller if the angle between the longitudinal axis of the fiber and the horizontal plane were 10°.

Errors due to the magnification can occur especially when PP is used as a matrix. PP has a tendency to form bubbles during the imbedding in the vacuum oven and the surface of the matrix disk becomes uneven. This rough surface of the PP disk causes optical disturbances and complicates the measurement of the fiber dimensions.

CONCLUSIONS

In this work we evaluated the applicability of the IFR method for measuring the interfacial tension between molten polymers, where PP served as matrix, and polyamides (PA6, PA66) and two thermotropic main-chain LCPs as fibers. With the method we were able to characterize the interfacial properties of PP/LCP and PP/PA blends and to rank the compatibilizers according to their effects on the blends.

The IFR method gave reproducible results with small standard deviations provided that the degree of thermal degradation was diminished by keeping the measuring time short. It was also important that the viscosities of the fiber and matrix should not be too different. Measured interfacial tensions were generally lower than the theoretical values calculated from the harmonic mean equation, but the order of the values for the different polymer pairs was similar. The measured interfacial tensions also correlated well with the morphology and properties of the blends. The reactive ethylene-based compatibilizer decreased the measured interfacial tension to 1/10 in both PA/PP and LCP/PP systems. According to our earlier studies this compatibilizer strongly modifies the morphology and properties of these blends leading, for example, to improved toughness.¹¹ The IFR measurements confirmed the enhanced interactions in these compatibilized blends indicated earlier by DSC, DMTA, and FTIR, and here by SEM. The interfacial properties of the materials could be characterized as was hoped, and the suitability of the blend components and compatibilizers could be evaluated without making the blends.

NOMENCLATURE

DMTA	Dynamic mechanical thermal analysis.
DSC	Differential scanning calorimetry.
FTIR	Fourier transform infrared spectroscopy.
HBA	<i>p</i> -Hydroxybenzoic acid.
HNA	6-Hydroxy-2-naphthoic acid.
IFR	Imbedded fiber retraction.
LCP	Liquid crystalline polymer.
MAH	Maleic anhydride.
PP	Polypropylene.
PA6	Polyamide 6, nylon 6.
PA66	Polyamide 66, nylon 66.
PC	Polycarbonate.
PET	Polyethylene terephthalate.

PMMA	Poly(methylene methacrylate).
PS	Polystyrene.
S/AN	Styrene/acrylonitrile copolymer.
S/AN/FN	Styrene/acrylonitrile/fumaronitrile terpolymer.
SEM	Scanning electron microscopy.
<i>A</i>	Interfacial area (m ²).
<i>d</i>	Diameter of the die (m).
<i>L</i>	Length of the fiber, length of the die (m).
<i>M_n</i>	Number average molecular weight (g/mol).
<i>M_w</i>	Weight average molecular weight (g/mol).
<i>r</i>	Dimensionless radius <i>r</i> .
<i>R(t)</i>	Effective radius of the fiber (m).
<i>R₀</i>	Final radius of the fiber (m).
<i>t</i>	Time (s).
<i>T</i>	Temperature (°C).
<i>x^p</i>	Polarity.

Greek Letters

γ_i	The surface tension of component <i>i</i> (mN/m).
γ_i^d	Dispersive part of the surface tension of component <i>i</i> (mN/m).
γ_i^p	Polar part of the surface tension of component <i>i</i> (mN/m).
γ_{12}	Interfacial tension between polymers 1 and 2 (mN/m).
η_e	Effective viscosity (Pa · s).
η_f	Viscosity of the fiber (Pa · s).
η_m	Viscosity of the matrix (Pa · s).
η_0	Zero-shear viscosity (Pa · s).
χ	Hydrodynamic coefficient.

REFERENCES

1. A. P. Plochocki, S. S. Dagli, and R. D. Andrews, *Polym. Eng. Sci.*, **30**, 741 (1990).
2. S. Wu, *Polym. Eng. Sci.*, **27**, 335 (1987).
3. S. Wu, in *Polymer Blends*, Vol. 1, D. R. Paul and S. Newman, Eds., Academic Press Inc., New York, 1978.
4. H. T. Patterson, K. H. Hu, T. H. Grindstaff, *J. Polym. Sci. C*, **34**, 31 (1974).
5. C. C. Chen and J. L. White, *Polym. Eng. Sci.*, **33**, 923 (1993).
6. S. Y. Hobbs, M. E. J. Dekkers, and V. H. Watkins, *Polymer*, **29**, 1598 (1988).
7. C. J. Carriere, A. Cohen, and C. B. Arends, *J. Rheol.*, **33**, 681 (1989).
8. A. Cohen and C. J. Carriere, *Rheol. Acta*, **28**, 223 (1989).

9. C. J. Carriere and A. Cohen, *J. Rheol.*, **35**, 205 (1991).
10. R. L. Sammler, R. P. Dion, C. J. Carriere, and A. Cohen, *Rheol. Acta*, **31**, 554 (1992).
11. R. M. Holsti-Miettinen, J. V. Seppälä, and O. T. Ikkala, *Polym. Eng. Sci.*, **32**, 868 (1992).
12. M. T. Heino and J. V. Seppälä, *J. Appl. Polym. Sci.*, **48**, 1677 (1993).
13. M. T. Heino, P. T. Hietaoja, T. P. Vainio, and J. V. Seppälä, *J. Appl. Polym. Sci.*, **51**, 259 (1994).
14. S. Wu, *Polymer Interface and Adhesion*, Marcel Dekker, New York, 1982.
15. P. K. H. Heidemeyer, Ph.D. dissertation, Rheinisch-Westfälische Technische Hochschule, Aachen, 1990.
16. S. Meretz, M. Kwiatkowski, and G. Hinrichsen, *Intern. Polym. Processing*, **VI**, 239 (1991).
17. F. J. Hybart and T. R. White, *J. Appl. Polym. Sci.*, **3**, 118 (1960).
18. S. S. Dagli, Ph.D. dissertation, Stevens Institute of Technology, New Jersey, 1991.
19. S. M. Guskey and H. H. Winter, *J. Rheol.*, **35**, 1191 (1991).

Received May 3, 1994

Accepted August 13, 1994